

Grant Free MIMO-NOMA with Differential Modulation for Machine Type Communications

Yuanyuan Zhang, Zhengdao Yuan, Qinghua Guo, *Senior Member, IEEE*, Zhongyong Wang, Jiangtao Xi, *Senior Member, IEEE*, Yanguang Yu and Yonghui Li, *Fellow, IEEE*

Abstract—This paper considers a challenging scenario of machine type communications, where we assume internet of things (IoT) devices send short packets sporadically to an access point (AP) and the devices are not synchronized in the packet level. High transmission efficiency and low latency are concerned. Motivated by the great potential of multiple-input multiple-output non-orthogonal multiple access (MIMO-NOMA) in massive access, we design a grant-free MIMO-NOMA scheme, and in particular differential modulation is used so that expensive channel estimation at the receiver (AP) can be bypassed. The receiver at AP needs to carry out active device detection and multi-device data detection. The active user detection is formulated as the estimation of the common support of sparse signals, and a message passing based sparse Bayesian learning (SBL) algorithm is designed to solve the problem. Due to the use of differential modulation, we investigate the problem of non-coherent multi-device data detection, and develop a message passing based Bayesian data detector, where the constraint of differential modulation is exploited to drastically improve the detection performance, compared to the conventional non-coherent detection scheme. Simulation results demonstrate the effectiveness of the proposed active device detector and non-coherent multi-device data detector.

Index Terms—Grant-free, non-orthogonal multiple access (NOMA), internet of things (IoT), multiple-input multiple-output (MIMO), message passing, machine type communications.

I. INTRODUCTION

AS an enabler for the Internet of Things (IoT), massive machine type communications have attracted much attention, which is characterized by massive connections and sporadic short-burst transmissions [1]–[3]. Due to the limited spectral resource, it is difficult to use the orthogonal multiple access (OMA) scheme to provide connectivity for a massive

number of IoT devices. Moreover, the conventional grant-based transmission schemes may incur uncertain latency and excessive signaling overhead due to the handshaking procedure, making the communications inefficient, especially in the case that IoT devices have only a small amount of payload data, e.g., a few bits for each transmission [4], [5]. The grant-free non-orthogonal multiple access (NOMA) [6]–[12], which uses a resource block to serve multiple users and does not need the handshaking procedure, is a very promising technique for machine type communications.

Recently, to further enhance the spectrum efficiency, multiuser access and/or communication reliability, NOMA has been combined with multiple-input and multiple-output (MIMO) [13]–[24], leading to MIMO-NOMA. In [14]–[22], with the assumption that the channel state information (CSI) is available to the receiver, the performance of MIMO-NOMA schemes and relevant signal processing techniques are studied. For practical applications, the CSI has to be acquired via training signals for coherent detection [23], [24]. However, due to the large number of variables to be estimated, the acquisition of accurate instantaneous CSI for (massive) MIMO leads to significant training overhead, and channel estimation is a challenging task, especially in the scenarios that wireless channels are fast time-varying. The implementation of grant-free MIMO-NOMA systems is even more challenging, but it has great intentional for massive machine type communications.

This paper deals with the design of grant-free MIMO-NOMA for machine type communications, where each device is equipped with a single antenna and the AP is equipped with a (massive) number of antennas. We assume that the data payload of the devices is small (e.g., a few bits), and the devices send information to an access point (AP) randomly. In addition, the data packet length of the devices is not fixed, so the devices are not synchronized in the packet level, i.e., any device is allowed to freely access the channel whenever it has information to transmit, and it becomes inactive when its packet is delivered. Due to the high flexibility of the transmissions and the consideration of high transmission efficiency, the realization of the system is very challenging, especially the implementation of the receiver at the AP, as it needs to identify the active devices and perform multi-device data detection. The conventional grant-free NOMA strategy is to first perform active user identification and channel estimation, followed by coherent data detection. However, due to a large number of antennas at the AP and the data packet of the devices is very short, the conventional strategy will render

Corresponding authors: Qinghua Guo and Zhongyong Wang.

Y. Zhang is with the School of Computer and Communication Engineering, Zhengzhou University of Light Industry, Zhengzhou 450002, Henan, China. She was with the School of Electrical, Computer and Telecommunications Engineering, University of Wollongong, Wollongong, NSW 2522, Australia (e-mail: ieyzhang@zzuli.edu.cn).

Z. Yuan is with the Artificial Intelligence Technology Engineering Research Center, Open University of Henan, and School of Information Engineering, Zhengzhou University, Zhengzhou 450002, China (e-mail: yuan_zhengdao@163.com).

Q. Guo, J. Xi and Y. Yu are with the School of Electrical, Computer and Telecommunications Engineering, University of Wollongong, Wollongong, NSW 2522, Australia (e-mail: qguo@uow.edu.au; jiangtao@uow.edu.au; yanguang@uow.edu.au).

Z. Wang is with the School of Information Engineering, Zhengzhou University, Zhengzhou 450001, China (e-mail: zywangzzu@gmail.com).

Y. Li is with the School of Electrical and Information Engineering, University of Sydney, Sydney, NSW 2006, Australia (e-mail: yonghui.li@sydney.edu.au).

the transmissions highly inefficient due to the requirement of long training signals for active user identification and channel estimation. Even the large training overhead is not an issue, it is unknown how to use the conventional strategy to handle the asynchronous transmissions of the IoT devices, where the devices have different packet lengths and are allowed to access and leave the channel freely.

In this work, we propose to solve the challenge by adopting differential modulation at the devices and designing non-coherent multi-device data detection at the AP. Such design can bypass channel estimation. The implementation of the transmitters is very simple, where each device is assigned a spreading sequence and transmits information with differential modulation. The receiver needs to first identify active users without the assistance of any training signals, and then performs multi-device data detection for the active users. We assume that the channels remain constant over two consecutive symbol intervals. The active user detection and multi-device data detection are performed symbol by symbol, so that the devices are allowed to access and leave the channel freely without packet level synchronization and channel estimation, which are the key to achieve high flexibility and high efficiency. To this end, the design of efficient active user detector and multi-device data detector is crucial. We use the factor graph and message passing techniques to address the problem. With the sparsity of active users, the active device detection is formulated as common support estimation of sparse signals, and we develop a message passing based sparse Bayesian learning (SBL) algorithm to solve it, where belief propagation (BP) [25] and mean field (MF) [26], [27] are combined to implement the SBL. After active users are identified, non-coherent data detection needs to be performed. For this, we investigate the problem of non-coherent multi-device detection problem and design a BP-MF message passing based data detector, which treats the differential modulation as a constraint and encodes it into a probabilistic form as a local function in the factor graph representation. We show that exploiting the constraint can improve the detection performance remarkably, compared to the conventional detection scheme. Simulation results are provided to demonstrate the effectiveness of the proposed scheme and superior performance of the developed algorithms.

The rest of this paper is organized as follows. In Section II, the grant free MIMO-NOMA system is designed and the problems of active device detection and non-coherent multi-device data detection are formulated. Message passing based non-coherent receiver is developed in Section III. Numerical simulation results are provided in Section IV, followed by conclusions in Section V.

Notation- Lowercase and uppercase letters denote scalars. Boldface lowercase and uppercase letters denote column vectors and matrices, respectively. The superscripts $(\cdot)^T$ and $(\cdot)^H$ denote the transpose and conjugate transpose operations, respectively, and α denotes equality of functions up to a scale factor. The function $\mathcal{CN}(x; \hat{x}, \sigma_x^2)$ stands for a complex Gaussian distribution with mean \hat{x} and variance σ_x^2 . As the convention, $\langle f(x, y, z) \rangle_{f(y)f(z)} = \iint f(x, y, z) f(y) f(z) dy dz$ is used to denote the marginalization operator. The expectation oper-

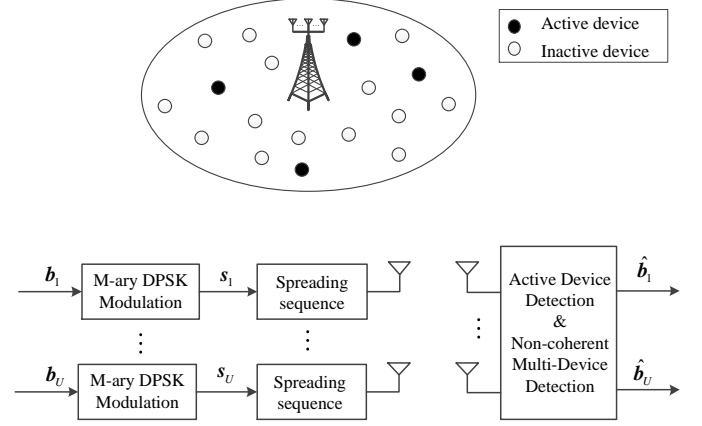


Fig. 1. Illustration and system diagram of grant-free MIMO-NOMA.

ator with respect to a scaled probability density function (PDF) $g(x)$ is expressed by $\langle x \rangle_{g(x)} = \int x g(x) dx / \int g(x') dx'$, and $\text{Var}[x]_{g(x)} = \langle |x|^2 \rangle_{g(x)} - |\langle x \rangle_{g(x)}|^2$ stands for the variance of x .

II. GRANT FREE MIMO-NOMA SYSTEM MODEL AND PROBLEM FORMULATION

A. Grant Free MIMO-NOMA with Differential Modulation

The grant free MIMO-NOMA system is illustrated in Fig. 1. We assume an IoT communication system, where an access point (AP) equipped with N antennas is used to serve U IoT devices, each equipped with a single antenna. In particular, we consider uplink transmission, i.e., the IoT devices send information to the AP. As the transmissions of the IoT devices are sporadic, i.e., not all devices are active at the same time, we use K to denote the number of active devices served by the AP.

Due to the small payload of the IoT devices, the requirement of low latency and (larger) number of antennas used at the AP, the use of training symbols for channel estimation and active device detection is not preferable. In this work, we design a non-coherent scheme and differential modulation is employed by the IoT devices, so that the use of training symbols can be avoided. As shown in Fig. 1 (b), the input bit stream \mathbf{b}_u of device u is mapped to a symbol sequence $\mathbf{s}_u = [s_{u,0}, s_{u,1}, \dots, s_{u,T-1}]$ with differential modulation, e.g., M-ary differential phase shift keying (DPSK), where T is the length of the symbol sequence and $s_{u,0}$ is a known reference symbol that is drawn from the M-ary DPSK constellation set \mathcal{X} . Then, each symbol in \mathbf{s}_u is spread onto L chips using a unique spreading sequence $\mathbf{p}_u \in \mathbb{C}^{L \times 1}$ for device u , which is a column of the spreading matrix $\mathbf{P} = [\mathbf{p}_1, \dots, \mathbf{p}_U]$. To support a large number of users with spreading sequences of limited length, the spreading sequences are not orthogonal. In this paper, the Zadoff-Chu (ZC) sequences [28], [29] with different roots and shifts are employed as the spreading sequences. As not all users are active, we define A_u as the activity indicator for device u , which takes 1 if the device is active, and 0 otherwise. The t -th equivalent transmitted symbol of device u is denoted as

$$\bar{s}_u^{(t)} = A_u s_{u,t}. \quad (1)$$

Then, the received signal at the n -th antenna can be expressed as

$$\mathbf{y}_n^{(t)} = \mathbf{P}\mathbf{H}_n\bar{\mathbf{s}}^{(t)} + \mathbf{w}_n^{(t)}, \quad (2)$$

where $\mathbf{y}_n^{(t)} \in \mathbb{C}^{L \times 1}$, $\mathbf{H}_n = \text{diag}(\mathbf{h}_n)$ is a diagonal matrix, whose diagonal elements are given as $\mathbf{h}_n = [h_{1,n}, h_{2,n}, \dots, h_{U,n}]$, $h_{u,n}$ is the channel coefficient between device u and the n -th antenna, which is complex Gaussian distributed with zero mean, $\bar{\mathbf{s}}^{(t)} = [\bar{s}_1^{(t)}, \bar{s}_2^{(t)}, \dots, \bar{s}_U^{(t)}]^T$ is the t -th transmitted equivalent symbol vector of length U , whose element $\bar{s}_u^{(t)}$ takes a value from the complex-constellation set $\bar{\mathcal{X}} \triangleq \{\mathcal{X} \cup 0\}$, and the noise vector on the n -th antenna $\mathbf{w}_n^{(t)} \sim \mathcal{CN}(\mathbf{w}_n^{(t)}; 0, \sigma_w^2 \mathbf{I}_L)$.

The received signals by N antennas can be expressed in a matrix form as

$$\mathbf{Y}^{(t)} = \mathbf{P} [\mathbf{H}_1\bar{\mathbf{s}}^{(t)}, \mathbf{H}_2\bar{\mathbf{s}}^{(t)}, \dots, \mathbf{H}_N\bar{\mathbf{s}}^{(t)}] + \mathbf{W}^{(t)}, \quad (3)$$

where $\mathbf{Y}^{(t)} = [\mathbf{y}_1^{(t)}, \mathbf{y}_2^{(t)}, \dots, \mathbf{y}_N^{(t)}]$ is a matrix of size $L \times N$, and $\mathbf{W} \in \mathbb{C}^{L \times N}$ is a matrix of white Gaussian noise whose power is unknown.

As mentioned before, the IoT devices are allowed to access and leave the channel freely as they may need to transmit their data to the AP randomly with varying packet length. By taking advantage of differential modulation, our aim is to obtain the transmitted information of active devices, while avoiding the estimation of the channel coefficients. To achieve this, both active device detection and data detection need to be carried out based on two consecutive received matrices $\mathbf{Y}^{(t)}$ and $\mathbf{Y}^{(t-1)}$, corresponding to two consecutive symbol intervals.

B. Problem Formulation

Define $\mathbf{x}_n^{(t)} = \mathbf{H}_n\bar{\mathbf{s}}^{(t)}$, where $\mathbf{x}_n^{(t)} = [x_{1,n}^{(t)}, x_{2,n}^{(t)}, \dots, x_{U,n}^{(t)}]^T$ is a vector of length U and $x_{u,n}^{(t)} = A_u h_{u,n} s_{u,t}$. From (3), we have

$$\mathbf{Y}^{(t)} = \mathbf{P}\mathbf{X}^{(t)} + \mathbf{W}^{(t)}, \quad (4)$$

where $\mathbf{X}^{(t)} = [\mathbf{x}_1^{(t)}, \mathbf{x}_2^{(t)}, \dots, \mathbf{x}_N^{(t)}]$ is an $U \times N$ matrix. As joint active device detection and data detection (multi-device detection) will lead to high complexity, we adopt a two-stage strategy, i.e., performing active device identification followed by data detection.

1) *Active Device Detection*: As only K out of U users are active, according to the definition of $\mathbf{X}^{(t)}$, we can see that each column of the matrix is a sparse vector, and all the columns share a common support. We need to find the non-zero rows of $\mathbf{X}^{(t)}$, then identify the spreading sequences of active users according to the indices of the non-zero rows (thereby active devices are detected). We define the common support of $\mathbf{X}^{(t)}$ as a set \mathcal{U}_a , whose elements are the indices of the non-zero rows of $\mathbf{X}^{(t)}$. Note that the cardinality of \mathcal{U}_a is the number of active users, i.e., $K = |\mathcal{U}_a|$. Hence active device detection can be formulated as a problem of recovering sparse vectors with a common support, and we will design a sparse Bayesian learning algorithm to solve it.

Based on the states of the devices over two consecutive symbol intervals, we can decide their activities. If a device is active at time $t-1$ while inactive at time t , the device finishes transmission. If a device is inactive at time $t-1$ while active at time t , the device just starts data transmission. If a device is

active at both time $t-1$ and time t , the device is transmitting data, and we need to perform data detection for the device.

2) *Non-Coherent Multi-Device Data Detection*: To facilitate multi-device data detection, we pick out the non-zero rows (whose indices belong to the support set \mathcal{U}_a) of $\mathbf{X}^{(t)}$ and $\mathbf{X}^{(t-1)}$, and the corresponding columns of \mathbf{P} . Then (4) can be reduced to

$$\mathbf{Y}^{(t)} = \bar{\mathbf{P}}\bar{\mathbf{X}}^{(t)} + \mathbf{W}^{(t)}, \quad (5)$$

where $\bar{\mathbf{P}}$ is an $L \times K$ matrix, whose columns are drawn from \mathbf{P} based on the support set \mathcal{U}_a , $\bar{\mathbf{X}}^{(t)}$ is a $K \times N$ matrix, whose rows are drawn from $\mathbf{X}^{(t)}$ based on the support set \mathcal{U}_a .

Assuming that DPSK is used, we define $\psi_k^{(t)} = s_{k,t}/s_{k,t-1}$ to denote the t -th symbol of device k . Then, we have

$$\begin{aligned} \psi_k^{(t)} &= \frac{s_{k,t}}{s_{k,t-1}} \\ &= \frac{x_{k,1}^{(t)}}{x_{k,1}^{(t-1)}} = \frac{h_{k,1}s_{k,t}}{h_{k,1}s_{k,t-1}} \\ &= \dots \\ &= \frac{x_{k,N}^{(t)}}{x_{k,N}^{(t-1)}} = \frac{h_{k,N}s_{k,t}}{h_{k,N}s_{k,t-1}}. \end{aligned} \quad (6)$$

In a vector form, the t -th symbol vector $\boldsymbol{\psi}^{(t)} = [\psi_1^{(t)}, \psi_2^{(t)}, \dots, \psi_K^{(t)}]^T$ over N antennas can be expressed as

$$\begin{aligned} \begin{bmatrix} \psi_1^{(t)} & \psi_1^{(t)} & \dots & \psi_1^{(t)} \\ \psi_2^{(t)} & \psi_2^{(t)} & \dots & \psi_2^{(t)} \\ \vdots & \vdots & \ddots & \vdots \\ \psi_K^{(t)} & \psi_K^{(t)} & \dots & \psi_K^{(t)} \end{bmatrix} &= \bar{\mathbf{X}}^{(t)} \oslash \bar{\mathbf{X}}^{(t-1)} \\ &= \begin{bmatrix} \frac{x_{1,1}^{(t)}}{x_{1,1}^{(t-1)}} & \frac{x_{1,2}^{(t)}}{x_{1,2}^{(t-1)}} & \dots & \frac{x_{1,N}^{(t)}}{x_{1,N}^{(t-1)}} \\ \frac{x_{2,1}^{(t)}}{x_{2,1}^{(t-1)}} & \frac{x_{2,2}^{(t)}}{x_{2,2}^{(t-1)}} & \dots & \frac{x_{2,N}^{(t)}}{x_{2,N}^{(t-1)}} \\ \vdots & \vdots & \ddots & \vdots \\ \frac{x_{K,1}^{(t)}}{x_{K,1}^{(t-1)}} & \frac{x_{K,2}^{(t)}}{x_{K,2}^{(t-1)}} & \dots & \frac{x_{K,N}^{(t)}}{x_{K,N}^{(t-1)}} \end{bmatrix}, \end{aligned} \quad (7)$$

where \oslash is the operation of element-wise division.

The multi-device data detection is formulated as the estimation of $\boldsymbol{\psi}^{(t)}$ based on $\mathbf{Y}^{(t)}$ and $\mathbf{Y}^{(t-1)}$. The conventional demodulation method carries out two steps: first estimate $\bar{\mathbf{X}}^{(t-1)}$ and $\bar{\mathbf{X}}^{(t)}$ based on $\mathbf{Y}^{(t-1)}$ and $\mathbf{Y}^{(t)}$, respectively, then use (7) to estimate $\{\psi_k^{(t)}\}$, based on which hard decision for the information bits can be performed. In this paper, we propose a new method, where the decision on $\{\psi_k^{(t)}\}$ is obtained directly based on $\mathbf{Y}^{(t-1)}$ and $\mathbf{Y}^{(t)}$ (instead of the intermediate results $\bar{\mathbf{X}}^{(t-1)}$ and $\bar{\mathbf{X}}^{(t)}$ as in the conventional two step approach), leading to remarkable performance gain as demonstrated later.

In this paper, both active device detection and multi-device data detection are solved with Bayesian methods. In particular, we use the factor graph techniques and design efficient message passing algorithms to solve the problems, which are elaborated in next section.

III. MESSAGE PASSING BASED BAYESIAN APPROACHES FOR ACTIVE DEVICE DETECTION AND NON-COHERENT MULTI-DEVICE DATA DETECTION

In this section, factor graph representations for the formulated problems are developed, based on which message passing-based Bayesian algorithms are designed for active device detection and multi-device data detection.

A. Graph Representation for Block SBL-Based Active Device Detection

To identify the active devices, we develop a block SBL method to estimate the common support of the row sparse matrix $\mathbf{X}^{(t)}$ in (4). Here, a two-layer hierarchical prior is employed, where the prior of the (n, u) -th element in $\mathbf{X}^{(t)}$ is

$$p(x_{u,n}^{(t)}) = \int p(x_{u,n}^{(t)}|\gamma_u)p(\gamma_u)d\gamma_u, \quad (8)$$

where $p(x_{u,n}^{(t)}|\gamma_u) = \mathcal{CN}(x_{u,n}^{(t)}; 0, \gamma_u^{-1})$, and $p(\gamma_u, \epsilon) = \text{Ga}(\gamma_u; \epsilon, \eta)$ with hyper-parameters ϵ and η . Due to the common support of the columns of $\mathbf{X}^{(t)}$, the elements of the u -th row in $\mathbf{X}^{(t)}$ share a single hyper-parameter precision γ_u , as shown in (8). The elements of $\mathbf{X}^{(t)}$ are conditionally independent, and we have

$$p(\mathbf{X}^{(t)}|\boldsymbol{\gamma}) = \prod_{n=1}^N \prod_{u=1}^U p(x_{u,n}^{(t)}|\gamma_u), \quad (9)$$

where $\boldsymbol{\gamma} = [\gamma_1, \gamma_2, \dots, \gamma_U]^T$. We assume that the noise precision at the n -th antenna λ_n is unknown, and an improper prior $p(\lambda_n) \propto 1/\lambda_n$ is assumed.

Then the joint distribution of $\mathbf{X}^{(t)}$, $\boldsymbol{\gamma}$ and $\boldsymbol{\lambda}$ can be expressed as

$$\begin{aligned} p(\mathbf{X}^{(t)}, \boldsymbol{\gamma}, \boldsymbol{\lambda}|\mathbf{Y}^{(t)}) \\ \propto p(\mathbf{Y}^{(t)}|\mathbf{X}^{(t)}, \boldsymbol{\lambda})p(\mathbf{X}^{(t)}|\boldsymbol{\gamma})p(\boldsymbol{\lambda})p(\boldsymbol{\gamma}) \\ = \prod_{u=1}^U p(\gamma_u) \prod_{n=1}^N \left(\prod_{l=1}^L \left(p(y_{l,n}^{(t)}|\mathbf{x}_n^{(t)}, \lambda_n) \right) p(\lambda_n) p(x_{u,n}^{(t)}|\gamma_u) \right), \end{aligned} \quad (10)$$

where $p(y_{l,n}^{(t)}|\mathbf{x}_n^{(t)}, \lambda_n) = \mathcal{CN}(y_{l,n}^{(t)}; \mathbf{p}_l^T \mathbf{x}_n^{(t)}, \lambda_n^{-1})$ with \mathbf{p}_l^T being the l -th row of \mathbf{P} and $\mathbf{x}_n^{(t)}$ being the n -th column of $\mathbf{X}^{(t)}$ in (4), and $\boldsymbol{\lambda} = [\lambda_1, \dots, \lambda_N]^T$.

To facilitate the factor graph representation of the factorization in (10), we introduce the notations in Table I, showing the correspondence between the factor labels and the underlying distributions they represent. In addition, to combine BP and MF message passing, we introduce the auxiliary variable $z_{l,n}^{(t)} = \mathbf{p}_l^T \mathbf{x}_n^{(t)}$ in Table I, inducing extra hard constraints $\delta(z_{l,n}^{(t)} - \mathbf{p}_l^T \mathbf{x}_n^{(t)})$, which is denoted by $f_{z_{l,n}}^{(t)}(z_{l,n}^{(t)}, \mathbf{x}_n^{(t)})$. Then $p(y_{l,n}^{(t)}|\mathbf{x}_n^{(t)}, \lambda_n)$ becomes a function with $z_{l,n}^{(t)}$ and λ_n as variables, i.e., $\mathcal{CN}(y_{l,n}^{(t)}; z_{l,n}^{(t)}, \lambda_n^{-1})$. The factor graph representation of (10) is shown in Fig. 2. The activity of device u is detected by comparing $\hat{\gamma}_u$ with a threshold.

B. Graph Representation for Bayesian Approach for Non-Coherent Multi-Device Data Detection

With the results of active device detection, multi-device data detection is then carried out based on (5). As differential

TABLE I
THE FACTORS INVOLVED IN THE FACTORIZATION IN (10)

Factor	Distribution	Functional Form
$f_{\lambda_n}(\lambda_n)$	$p(\lambda_n)$	$1/\lambda_n$
$f_{y_{l,n}}^{(t)}(z_{l,n}^{(t)}, \lambda_n)$	$p(y_{l,n}^{(t)} z_{l,n}^{(t)}, \lambda_n)$	$\mathcal{CN}(y_{l,n}^{(t)}; z_{l,n}^{(t)}, \lambda_n^{-1})$
$f_{z_{l,n}}^{(t)}(z_{l,n}^{(t)}, \mathbf{x}_n^{(t)})$	$p(z_{l,n}^{(t)} \mathbf{x}_n^{(t)})$	$\delta(z_{l,n}^{(t)} - \mathbf{p}_l^T \mathbf{x}_n^{(t)})$
$f_{x_{u,n}}^{(t)}(x_{u,n}^{(t)}, \gamma_u)$	$p(x_{u,n}^{(t)} \gamma_u)$	$\mathcal{CN}(x_{u,n}^{(t)}; 0, \gamma_u^{-1})$
$f_{\gamma_u}(\gamma_u, \epsilon)$	$p(\gamma_u, \epsilon)$	$\text{Ga}(\gamma_u; \epsilon, \eta)$

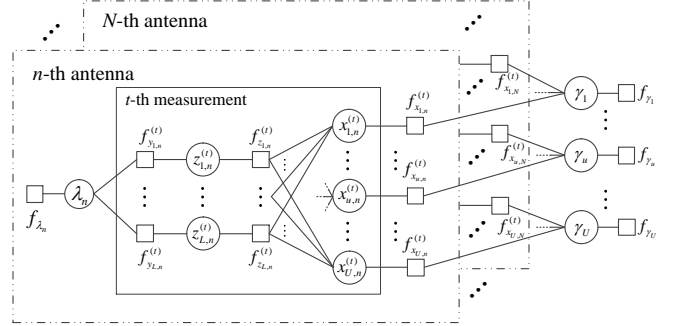


Fig. 2. Factor graph representation of (10).

modulation is used to avoid the training process, for the detection of the symbols of the active devices at time t , the received signal $\mathbf{Y}^{(t-1)}$ at time $t-1$ is also required. In the design of our Bayesian approach, the differential modulation, i.e., the relationship between $\mathbf{X}^{(t)}$ and $\mathbf{X}^{(t-1)}$ in (7) is regarded as a hard constraint. We transform it into a probabilistic form, and then the joint distribution of $\bar{\mathbf{X}}^{(t)}$, $\bar{\mathbf{X}}^{(t-1)}$ and $\boldsymbol{\psi}^{(t)}$ can be expressed as

$$p(\bar{\mathbf{X}}^{(t)}, \bar{\mathbf{X}}^{(t-1)}, \boldsymbol{\psi}^{(t)}) = \prod_{k=1}^K p(\psi_k^{(t)}) \prod_{n=1}^N p(\bar{x}_{k,n}^{(t)}, \bar{x}_{k,n}^{(t-1)}|\psi_k^{(t)}), \quad (11)$$

where $p(\bar{x}_{k,n}^{(t)}, \bar{x}_{k,n}^{(t-1)}|\psi_k^{(t)})$ represents a hard constraint, i.e., $\delta(\bar{x}_{k,n}^{(t)} - \psi_k^{(t)} \bar{x}_{k,n}^{(t-1)})$, and $p(\psi_k^{(t)})$ is the prior of $\psi_k^{(t)}$. As $\psi_k^{(t)}$ is discrete valued, we have $p(\psi_k^{(t)}) = \sum_{q \in \mathcal{X}_d} \frac{1}{Q} \delta(\psi_k^{(t)} - q)$, and Q is the cardinality of the demodulation symbol set \mathcal{X}_d , i.e. $Q = |\mathcal{X}_d|$. Given $\mathbf{Y}^{(t)}$ and $\mathbf{Y}^{(t-1)}$, the joint a posteriori distribution of $\bar{\mathbf{X}}^{(t)}$, $\bar{\mathbf{X}}^{(t-1)}$, $\boldsymbol{\psi}^{(t)}$ and $\boldsymbol{\lambda}$ can be expressed as

$$\begin{aligned} p(\bar{\mathbf{X}}^{(t)}, \bar{\mathbf{X}}^{(t-1)}, \boldsymbol{\psi}, \boldsymbol{\lambda}|\mathbf{Y}^{(t)}, \mathbf{Y}^{(t-1)}) \\ \propto p(\mathbf{Y}^{(t)}|\bar{\mathbf{X}}^{(t)}, \boldsymbol{\lambda})p(\mathbf{Y}^{(t-1)}|\bar{\mathbf{X}}^{(t-1)}, \boldsymbol{\lambda})p(\bar{\mathbf{X}}^{(t)}, \bar{\mathbf{X}}^{(t-1)}, \boldsymbol{\psi})p(\boldsymbol{\lambda}) \\ = \prod_{k=1}^K p(\psi_k^{(t)}) \prod_{n=1}^N \left(\prod_{l=1}^L \left(p(y_{l,n}^{(t)}|\bar{\mathbf{x}}_n^{(t)}, \lambda_n) p(y_{l,n}^{(t-1)}|\bar{\mathbf{x}}_n^{(t-1)}, \lambda_n) \right) \right. \\ \left. \cdot p(\lambda_n) p(\bar{x}_{k,n}^{(t)}, \bar{x}_{k,n}^{(t-1)}|\psi_k^{(t)}) \right), \end{aligned} \quad (12)$$

where $p(y_{l,n}^{(t)}|\bar{\mathbf{x}}_n^{(t)}, \lambda_n) = \mathcal{CN}(y_{l,n}^{(t)}; \bar{\mathbf{p}}_l^T \bar{\mathbf{x}}_n^{(t)}, \lambda_n^{-1})$ with $\bar{\mathbf{p}}_l^T$ being the l -th row of $\bar{\mathbf{P}}$, and $\bar{\mathbf{x}}_n^{(t)}$ being the n -th column of $\bar{\mathbf{X}}^{(t)}$ in (5).

To facilitate the factor graph representation of the factorization in (12), we introduce the notations in Table II. In addition,

TABLE II
THE FACTORS INVOLVED IN THE FACTORIZATION IN (12)

Factor	Distribution	Functional Form
$f_{\lambda_n}(\lambda_n)$	$p(\lambda_n)$	$1/\lambda_n$
$f_{y_{l,n}}^{(t)}(z_{l,n}^{(t)}, \lambda_n)$	$p(y_{l,n}^{(t)} z_{l,n}^{(t)}, \lambda_n)$	$\mathcal{CN}(y_{l,n}^{(t)}; z_{l,n}^{(t)}, \lambda_n^{-1})$
$f_{z_{l,n}}^{(t)}(z_{l,n}^{(t)}, \bar{\mathbf{x}}_n^{(t)})$	$p(z_{l,n}^{(t)} \bar{\mathbf{x}}_n^{(t)})$	$\delta(z_{l,n}^{(t)} - \bar{\mathbf{p}}_l^T \bar{\mathbf{x}}_n^{(t)})$
$f_{\delta_{k,n}}^{(t)}(\bar{x}_{k,n}^{(t)}, \bar{x}_{k,n}^{(t-1)}, \psi_k^{(t)})$	$p(\bar{x}_{k,n}^{(t)}, \bar{x}_{k,n}^{(t-1)} \psi_k^{(t)})$	$\delta(\bar{x}_{k,n}^{(t)} - \psi_k^{(t)} \bar{x}_{k,n}^{(t-1)})$
$f_{\psi_k^{(t)}}(\psi_k^{(t)})$	$p(\psi_k^{(t)})$	$\sum_{q \in \mathcal{X}} \frac{1}{Q} \delta(\psi_k^{(t)} - q)$

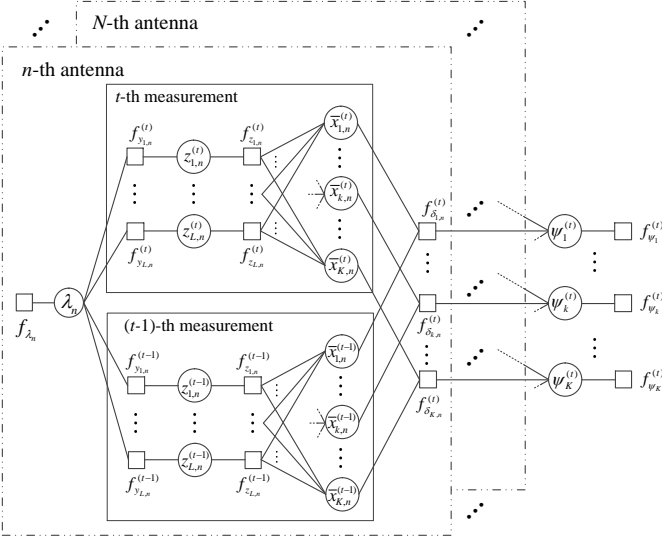


Fig. 3. Factor graph representation of (12).

we introduce the auxiliary variable $z_{l,n}^{(t)} = \bar{\mathbf{p}}_l^T \bar{\mathbf{x}}_n^{(t)}$ in Table II, inducing extra hard constraints $\delta(z_{l,n}^{(t)} - \bar{\mathbf{p}}_l^T \bar{\mathbf{x}}_n^{(t)})$, which is denoted by $f_{z_{l,n}}^{(t)}(z_{l,n}^{(t)}, \bar{\mathbf{x}}_n^{(t)})$. The stretched factor graph representation of (12) is shown in Fig.3. It is noted that the size of the factor graph in Fig.3 is much smaller than that in Fig.2 because the inactive users have been removed, leading to significant advantage in terms of computational complexity, compared to the strategy of joint active device detection and data detection.

C. Message Passing Algorithm for Active Device Detection

We detail the forward (from left to right) and backward (from right to left) message computations at each node of Fig. 2 for active device detection, where some approximations are introduced to reduce the computational complexity. We use $I_{A \rightarrow B}(x)$ to denote a message passed from a variable node (function node) A to a function node (variable node) B , which is a function of x . The notations m and v are used to denote the mean and variance of a Gaussian message specified by their subscripts. The arrows over m and v represent the directions of Gaussian message passing. Note that, if a forward message computation requires backward messages, we use the messages in previous iteration by default.

In Fig. 2, combined BP and MF based message passing is used to realize the estimation of $\{\gamma_u, \forall u\}$, where

the function nodes $\{f_{y_{l,n}}^{(t)}(z_{l,n}^{(t)}, \lambda_n), \forall l, n\}$, $\{f_{y_{l,n}}^{(t-1)}(z_{l,n}^{(t-1)}, \lambda_n), \forall l, n\}$, $\{f_{x_{u,n}}^{(t)}(x_{u,n}^{(t)}, \gamma_u), \forall u, n\}$ and $\{f_{x_{u,n}}^{(t-1)}(x_{u,n}^{(t-1)}, \gamma_u), \forall u, n\}$ are handled by the MF rule, and the function nodes $\{f_{z_{l,n}}^{(t)}, \forall l, n\}$ and $\{f_{z_{l,n}}^{(t-1)}, \forall l, n\}$ are handled by the BP rules. We note that some proper message approximations are used to reduce the computational complexity.

1) *Forward message computations:* With the belief $b(\lambda_n)$ whose computation is delayed to (41), the outgoing forward message at $f_{y_{l,n}}^{(t)}$ can be expressed as

$$I_{f_{y_{l,n}}^{(t)} \rightarrow z_{l,n}^{(t)}}(z_{l,n}^{(t)}) \propto \exp \left\{ \int \ln \left[f_{y_{l,n}}^{(t)}(\lambda_n, z_{l,n}^{(t)}) \right] b(\lambda_n) d\lambda_n \right\} \propto \mathcal{CN}(z_{l,n}^{(t)}; y_{l,n}^{(t)}, \hat{\lambda}_n^{-1}), \quad (13)$$

where $\hat{\lambda}_n$ is calculated in (42). With $I_{z_{l,n}^{(t)} \rightarrow f_{z_{l,n}}^{(t)}}(z_{l,n}^{(t)}) = I_{f_{y_{l,n}}^{(t)} \rightarrow z_{l,n}^{(t)}}(z_{l,n}^{(t)})$ and $\{I_{x_{u',n}^{(t)} \rightarrow f_{z_{l,n}}^{(t)}}(x_{u',n}^{(t)}), \forall u' \neq u\}$ computed in (31), the outgoing forward message at $f_{z_{l,n}}^{(t)}$ can be expressed as

$$I_{f_{z_{l,n}}^{(t)} \rightarrow x_{u,n}^{(t)}}(x_{u,n}^{(t)}) = \int f_{z_{l,n}}^{(t)}(z_{l,n}^{(t)}, \bar{\mathbf{x}}_n^{(t)}) I_{z_{l,n}^{(t)} \rightarrow f_{z_{l,n}}^{(t)}}(z_{l,n}^{(t)}) \cdot \prod_{u' \neq u} I_{x_{u',n}^{(t)} \rightarrow f_{z_{l,n}}^{(t)}}(x_{u',n}^{(t)}) dz_{l,n}^{(t)} d\bar{\mathbf{x}}_n^{(t)} \backslash x_{u,n}^{(t)} \propto \mathcal{CN}(x_{u,n}^{(t)}; \bar{m}_{x_{u,n}^{(t)}}^{(t)}, \bar{v}_{x_{u,n}^{(t)}}^{(t)}), \quad (14)$$

where

$$\bar{m}_{x_{u,n}^{(t)}}^{(t)} = \frac{y_{l,n}^{(t)} - \bar{m}_{z_{l,n}^{(t)}}^{(t)} + P_{l,u} \bar{m}_{x_{u,n}^{(t)}}^{(t)}}{P_{l,u}}, \quad (15)$$

$$\bar{v}_{x_{u,n}^{(t)}}^{(t)} = \frac{\hat{\lambda}_n^{-1} + \bar{v}_{z_{l,n}^{(t)}}^{(t)} - |P_{l,u}|^2 \bar{v}_{x_{u,n}^{(t)}}^{(t)}}{|P_{l,u}|^2}, \quad (16)$$

and

$$\bar{m}_{z_{l,n}^{(t)}}^{(t)} = \sum_{u=1}^U P_{l,u} \bar{m}_{x_{u,n}^{(t)}}^{(t)}, \quad (17)$$

$$\bar{v}_{z_{l,n}^{(t)}}^{(t)} = \sum_{u=1}^U |P_{l,u}|^2 \bar{v}_{x_{u,n}^{(t)}}^{(t)}. \quad (18)$$

Thus, with $\{I_{f_{z_{l,n}}^{(t)} \rightarrow x_{u,n}^{(t)}}(x_{u,n}^{(t)}), \forall l\}$, the outgoing forward message at $x_{u,n}^{(t)}$ reads

$$I_{x_{u,n}^{(t)} \rightarrow f_{x_{u,n}}^{(t)}}(x_{u,n}^{(t)}) = \prod_{l=1}^L I_{f_{z_{l,n}}^{(t)} \rightarrow x_{u,n}^{(t)}}(x_{u,n}^{(t)}) \propto \mathcal{CN}(x_{u,n}^{(t)}; \bar{m}_{x_{u,n}^{(t)}}^{(t)}, \bar{v}_{x_{u,n}^{(t)}}^{(t)}), \quad (19)$$

where

$$\bar{v}_{x_{u,n}^{(t)}}^{(t)} = \left(\sum_{l=1}^L \frac{1}{\bar{v}_{x_{u,n}^{(t)}}^{(t)}} \right)^{-1} \approx \left(\sum_{l=1}^L \frac{|P_{l,u}|^2}{\hat{\lambda}_n^{-1} + \bar{v}_{z_{l,n}^{(t)}}^{(t)}} \right)^{-1}, \quad (20)$$

$$\bar{m}_{x_{u,n}^{(t)}}^{(t)} \approx \bar{v}_{x_{u,n}^{(t)}}^{(t)} \sum_{l=1}^L \frac{P_{l,u}^H (y_{l,n}^{(t)} - \bar{m}_{z_{l,n}^{(t)}}^{(t)})}{\hat{\lambda}_n^{-1} + \bar{v}_{z_{l,n}^{(t)}}^{(t)}} + m_{x_{u,n}^{(t)}}^{(t)}, \quad (21)$$

and the derivation of (21) is provided in Appendix A. With $I_{x_{u,n} \rightarrow f_{x_{u,n}}}^{(t)}(x_{u,n})$ and $I_{f_{x_{u,n}} \rightarrow x_{u,n}}^{(t)}(x_{u,n})$ given in (30), the belief of $x_{u,n}^{(t)}$ can be updated as

$$b(x_{u,n}^{(t)}) = I_{x_{u,n} \rightarrow f_{x_{u,n}}}^{(t)}(x_{u,n}) I_{f_{x_{u,n}} \rightarrow x_{u,n}}^{(t)}(x_{u,n}) \propto \mathcal{CN}(x_{u,n}^{(t)}; m_{x_{u,n}}^{(t)}, v_{x_{u,n}}^{(t)}), \quad (22)$$

where

$$m_{x_{u,n}}^{(t)} = \frac{\vec{m}_{x_{u,n}}^{(t)}}{1 + \hat{\gamma}_u v_{x_{u,n}}^{(t)}}, \quad (23)$$

$$v_{x_{u,n}}^{(t)} = \left(\frac{1}{\vec{v}_{x_{u,n}}^{(t)}} + \hat{\gamma}_u \right)^{-1}, \quad (24)$$

and $\hat{\gamma}_u$ is given by (27). Thus, the outgoing forward message at $f_{x_{u,n}}^{(t)}$ can be computed as

$$I_{f_{x_{u,n}} \rightarrow \gamma_u}(\gamma_u) \propto \exp \left\{ \int \ln [f_{x_{u,n}}^{(t)}(x_{u,n}, \gamma_u)] b(x_{u,n}^{(t)}) dx_{u,n}^{(t)} \right\} \propto \gamma_u \exp \left\{ -\gamma_u \left(|m_{x_{u,n}}^{(t)}|^2 + v_{x_{u,n}}^{(t)} \right) \right\}. \quad (25)$$

With $\{I_{f_{x_{u,n}} \rightarrow \gamma_u}^{(t)}(\gamma_u), \forall u, n\}$ and $I_{f_{\gamma_u} \rightarrow \gamma_u}(\gamma_u)$ computed in (29), the belief of γ_u can be updated as

$$b(\gamma_u) = I_{f_{\gamma_u} \rightarrow \gamma_u}(\gamma_u) \prod_{n=1}^N I_{f_{x_{u,n}} \rightarrow \gamma_u}^{(t)}(\gamma_u) \propto \gamma_u^{\hat{\epsilon}+N-1} \exp \left\{ -\gamma_u \left[\eta + \sum_{n=1}^N (|m_{x_{u,n}}^{(t)}|^2 + v_{x_{u,n}}^{(t)}) \right] \right\}. \quad (26)$$

Thus, the estimation of γ_u can be updated by

$$\hat{\gamma}_u = \langle \gamma_u \rangle_{b(\gamma_u)} = \frac{\hat{\epsilon} + N}{\eta + \sum_{n=1}^N (|m_{x_{u,n}}^{(t)}|^2 + v_{x_{u,n}}^{(t)})}. \quad (27)$$

According to the results in [30], to enhance the performance of SBL, we can set $\eta = 0$, and update ϵ automatically, i.e.,

$$\hat{\epsilon} = \frac{1}{2} \sqrt{\log \left(\frac{1}{U} \sum_u \hat{\gamma}_u \right) - \frac{1}{U} \sum_u \log \hat{\gamma}_u}. \quad (28)$$

2) *Backward message computations:* According to the MF rule, the outgoing backward message at f_{γ_u} can be calculated by

$$I_{f_{\gamma_u} \rightarrow \gamma_u}(\gamma_u) \propto \exp \left\{ \int \ln [f_{\gamma_u}(\gamma_u, \epsilon)] b(\epsilon) d\epsilon \right\} \propto Ga(\gamma_u; \hat{\epsilon}, \eta). \quad (29)$$

With $b(\gamma_u)$, the outgoing backward message at $f_{x_{u,n}}^{(t)}$ can be computed as

$$I_{f_{x_{u,n}} \rightarrow x_{u,n}}^{(t)}(x_{u,n}) \propto \exp \left\{ \int \ln [f_{x_{u,n}}^{(t)}(x_{u,n}, \gamma_u)] b(\gamma_u) d\gamma_u \right\} \propto \mathcal{CN}(x_{u,n}^{(t)}; 0, \hat{\gamma}_u^{-1}). \quad (30)$$

With the calculated $I_{f_{z_{l,n}}^{(t)} \rightarrow x_{u,n}}^{(t)}(x_{u,n})$ in (14) and $b(x_{u,n}^{(t)})$ in (22), the outgoing backward message at $x_{u,n}^{(t)}$ is given as

$$I_{x_{u,n} \rightarrow f_{z_{l,n}}^{(t)}}(x_{u,n}^{(t)}) = \frac{b(x_{u,n}^{(t)})}{I_{f_{z_{l,n}}^{(t)} \rightarrow x_{u,n}}^{(t)}(x_{u,n}^{(t)})} \propto \mathcal{CN}(x_{u,n}^{(t)}; \bar{m}_{x_{u,n,l}}^{(t)}, \bar{v}_{x_{u,n,l}}^{(t)}), \quad (31)$$

where

$$\bar{v}_{x_{u,n,l}}^{(t)} = \left(\frac{1}{v_{x_{u,n}}^{(t)}} - \frac{1}{\vec{v}_{x_{u,n,l}}^{(t)}} \right)^{-1} \approx v_{x_{u,n}}^{(t)}, \quad (32)$$

and

$$\begin{aligned} \bar{m}_{x_{u,n,l}}^{(t)} &= \bar{v}_{x_{u,n,l}}^{(t)} \left(\frac{m_{x_{u,n}}^{(t)}}{v_{x_{u,n}}^{(t)}} - \frac{\vec{m}_{x_{u,n,l}}^{(t)}}{\vec{v}_{x_{u,n,l}}^{(t)}} \right) \\ &\stackrel{(32)}{\approx} m_{x_{u,n}}^{(t)} - v_{x_{u,n}}^{(t)} \frac{\vec{m}_{x_{u,n,l}}^{(t)}}{\vec{v}_{x_{u,n,l}}^{(t)}}. \end{aligned} \quad (33)$$

With $\{I_{x_{u,n} \rightarrow f_{z_{l,n}}^{(t)}}^{(t)}(x_{u,n}^{(t)}), \forall u\}$, the outgoing backward message at $f_{z_{l,n}}^{(t)}$ can be expressed as

$$I_{f_{z_{l,n}}^{(t)} \rightarrow z_{l,n}^{(t)}}(z_{l,n}^{(t)}) = \int f_{z_{l,n}}^{(t)}(z_{l,n}^{(t)}, \mathbf{x}_n^{(t)}) \prod_{u=1}^U I_{x_{u,n} \rightarrow f_{z_{l,n}}^{(t)}}^{(t)}(x_{u,n}^{(t)}) d\mathbf{x}_n^{(t)} \propto \mathcal{CN}(z_{l,n}^{(t)}; \bar{m}_{z_{l,n}}^{(t)}, \bar{v}_{z_{l,n}}^{(t)}), \quad (34)$$

where

$$\bar{v}_{z_{l,n}}^{(t)} = \sum_{u=1}^U |P_{l,u}|^2 \bar{v}_{x_{u,n,l}}^{(t)} \stackrel{(32)}{\approx} \sum_{u=1}^U |P_{l,u}|^2 v_{x_{u,n}}^{(t)}, \quad (35)$$

$$\bar{m}_{z_{l,n}}^{(t)} \approx \sum_{u=1}^U P_{l,u} m_{x_{u,n}}^{(t)} - \frac{\bar{v}_{z_{l,n}}^{(t)} (y_{l,n}^{(t)} - i^{-1} \bar{m}_{z_{l,n}}^{(t)})}{\hat{\lambda}_n^{-1} + i^{-1} \bar{v}_{z_{l,n}}^{(t)}}, \quad (36)$$

and the derivation of (36) is provided in Appendix A. Note that, to update $\bar{m}_{z_{l,n}}^{(t)}$, we need $\bar{v}_{z_{l,n}}^{(t)}$ and $\bar{m}_{z_{l,n}}^{(t)}$ in the previous iteration, so the superscript $i-1$ is introduced to differentiate them. With $I_{f_{z_{l,n}}^{(t)} \rightarrow z_{l,n}^{(t)}}^{(t)}(z_{l,n}^{(t)})$ and $I_{f_{\gamma_{l,n}} \rightarrow z_{l,n}^{(t)}}^{(t)}(z_{l,n}^{(t)})$ computed in (13), the belief of $z_{l,n}^{(t)}$ can be updated as

$$b(z_{l,n}^{(t)}) = I_{f_{\gamma_{l,n}} \rightarrow z_{l,n}^{(t)}}^{(t)}(z_{l,n}^{(t)}) I_{f_{z_{l,n}}^{(t)} \rightarrow z_{l,n}^{(t)}}^{(t)}(z_{l,n}^{(t)}) \propto \mathcal{CN}(z_{l,n}^{(t)}; m_{z_{l,n}}^{(t)}, v_{z_{l,n}}^{(t)}), \quad (37)$$

where

$$v_{z_{l,n}}^{(t)} = \left(\hat{\lambda}_n + \frac{1}{\bar{v}_{z_{l,n}}^{(t)}} \right)^{-1}, \quad (38)$$

$$m_{z_{l,n}}^{(t)} = v_{z_{l,n}}^{(t)} \left(y_{l,n}^{(t)} \hat{\lambda}_n + \frac{\bar{m}_{z_{l,n}}^{(t)}}{\bar{v}_{z_{l,n}}^{(t)}} \right). \quad (39)$$

Thus, the outgoing backward message at $f_{y_{l,n}}^{(t)}$ is given by

$$I_{f_{y_{l,n}}^{(t)} \rightarrow \lambda_n}(\lambda_n) \propto \exp \left\{ \int \ln \left[f_{y_{l,n}}^{(t)}(\lambda_n, z_{l,n}^{(t)}) \right] b(z_{l,n}^{(t)}) dz_{l,n}^{(t)} \right\} \\ \propto \lambda_n \exp \left\{ -\lambda_n \left(|m_{z_{l,n}}^{(t)} - y_{l,n}^{(t)}|^2 + v_{z_{l,n}}^{(t)} \right) \right\}. \quad (40)$$

With $\{I_{f_{y_{l,n}}^{(t)} \rightarrow \lambda_n}(\lambda_n), \forall l\}$ and the a prior $f_{\lambda_n}(\lambda_n)$, the belief of λ_n can be updated by

$$b(\lambda_n) = f_{\lambda_n}(\lambda_n) \prod_{l=1}^L I_{f_{y_{l,n}}^{(t)} \rightarrow \lambda_n}(\lambda_n) \\ \propto \lambda_n^{L-1} \exp \left\{ -\lambda_n \sum_{l=1}^L \left(|m_{z_{l,n}}^{(t)} - y_{l,n}^{(t)}|^2 + v_{z_{l,n}}^{(t)} \right) \right\}. \quad (41)$$

Thus, the estimation of noise precision is given as

$$\hat{\lambda}_n = \langle \lambda_n \rangle_{b_{\lambda_n}(\lambda_n)} = \frac{L}{\sum_{l=1}^L \left(|m_{z_{l,n}}^{(t)} - y_{l,n}^{(t)}|^2 + v_{z_{l,n}}^{(t)} \right)}. \quad (42)$$

The BP-MF message passing algorithm (BP-MF-MPA) for active device detection is summarized in Algorithm 1. The estimated hyper-parameter $\{\hat{y}_u, \forall u\}$ is used to detect the activity of device u by comparing it with a threshold G_{th} (which can be calculated as [31]), so we have $\mathcal{I}_a = \text{find}(\{\hat{y}_u\} < G_{th})$.

D. Message Passing Algorithm for Non-Coherent Multi-Device Detection

It is worth mentioning that Fig. 3 is obtained based on Fig. 2, where the variable nodes associated with inactive devices are removed, and the differential modulation constrains are added. BP and MF message passing is used to realize the estimation of $\{\psi_k, \forall k\}$. The message computations of the function nodes $\{f_{y_{l,n}}^{(t)}(z_{l,n}^{(t)}, \lambda_n), \forall l, n\}$ and $\{f_{z_{l,n}}^{(t)}, \forall l, n\}$ are similar to those in Fig. 2, which are omitted in this section. The function nodes $\{f_{\delta_{k,n}}^{(t)}(\bar{x}_{k,n}^{(t)}, \bar{x}_{k,n}^{(t-1)}, \psi_k^{(t)}), \forall k, n\}$ are handled by the BP rule, and some messages are approximated to be Gaussian based on moment matching to make the message passing tractable. As the message computation for the $(t-1)$ -th measurement is similar to that for the t -th, we just detail the message computation for t -th measurement.

1) *Forward message computations:* Similar to (13) - (21), we have

$$I_{\bar{x}_{k,n}^{(t)} \rightarrow f_{\delta_{k,n}}^{(t)}}(\bar{x}_{k,n}^{(t)}) \propto \mathcal{CN}(\bar{x}_{k,n}^{(t)}; \vec{m}_{\bar{x}_{k,n}^{(t)}}^{(t)}, \vec{v}_{\bar{x}_{k,n}^{(t)}}^{(t)}), \quad (43)$$

where

$$\vec{v}_{\bar{x}_{k,n}^{(t)}} \approx \left(\sum_{l=1}^L \frac{|\bar{P}_{lk}|^2}{\hat{\lambda}_n^{-1} + \vec{v}_{z_{l,n}}^{(t)}} \right)^{-1}, \quad (44)$$

and

$$\vec{m}_{\bar{x}_{k,n}^{(t)}} \approx \vec{v}_{\bar{x}_{k,n}^{(t)}} \sum_{l=1}^L \frac{\bar{P}_{lk} (y_{l,n}^{(t)} - \vec{m}_{z_{l,n}}^{(t)})}{\hat{\lambda}_n^{-1} + \vec{v}_{z_{l,n}}^{(t)}} + m_{\bar{x}_{k,n}}^{(t)}. \quad (45)$$

With $I_{\bar{x}_{k,n}^{(t)} \rightarrow f_{\delta_{k,n}}^{(t)}}(\bar{x}_{k,n}^{(t)})$ and $I_{\bar{x}_{k,n}^{(t-1)} \rightarrow f_{\delta_{k,n}}^{(t)}}(\bar{x}_{k,n}^{(t-1)})$, the outgoing forward message at $f_{\delta_{k,n}}^{(t)}$ can be computed as

$$I_{f_{\delta_{k,n}}^{(t)} \rightarrow \psi_k^{(t)}}(\psi_k^{(t)}) = \int f_{\delta_{k,n}}^{(t)}(\bar{x}_{k,n}^{(t)}, \psi_k^{(t)}) I_{\bar{x}_{k,n}^{(t)} \rightarrow f_{\delta_{k,n}}^{(t)}}(\bar{x}_{k,n}^{(t)}) \\ \cdot I_{\bar{x}_{k,n}^{(t-1)} \rightarrow f_{\delta_{k,n}}^{(t)}}(\bar{x}_{k,n}^{(t-1)}) d\bar{x}_{k,n}^{(t)} d\bar{x}_{k,n}^{(t-1)} \quad (46) \\ = \mathcal{CN}(\vec{m}_{\bar{x}_{k,n}^{(t)}}; \psi_k^{(t)} \vec{m}_{\bar{x}_{k,n}^{(t-1)}}, \vec{v}_{\bar{x}_{k,n}^{(t)}} + |\psi_k^{(t)}|^2 \vec{v}_{\bar{x}_{k,n}^{(t-1)}}).$$

With $\{I_{f_{\delta_{k,n}}^{(t)} \rightarrow \psi_k^{(t)}}(\psi_k^{(t)}), \forall n\}$ and the a prior $f_{\psi_k}(\psi_k^{(t)})$, the belief of $\psi_k^{(t)}$ is given as

$$b(\psi_k^{(t)}) = f_{\psi_k}(\psi_k^{(t)}) \prod_{n=1}^N I_{f_{\delta_{k,n}}^{(t)} \rightarrow \psi_k^{(t)}}(\psi_k^{(t)}) \triangleq \sum_{q \in \mathcal{X}_d} \beta_{k,t}^q \delta(\psi_k^{(t)} - q), \quad (47)$$

where

$$\beta_{k,t}^q = \frac{\prod_{n=1}^N \mathcal{CN}(\vec{m}_{\bar{x}_{k,n}^{(t)}}; q \vec{m}_{\bar{x}_{k,n}^{(t-1)}}, \vec{v}_{\bar{x}_{k,n}^{(t)}} + |q|^2 \vec{v}_{\bar{x}_{k,n}^{(t-1)}})}{\sum_{q' \in \mathcal{X}_d} \prod_{n=1}^N \mathcal{CN}(\vec{m}_{\bar{x}_{k,n}^{(t)}}; q' \vec{m}_{\bar{x}_{k,n}^{(t-1)}}, \vec{v}_{\bar{x}_{k,n}^{(t)}} + |q'|^2 \vec{v}_{\bar{x}_{k,n}^{(t-1)}})} \quad (48)$$

2) *Backward message computations:* With the messages $\{I_{f_{\delta_{k,n'}}^{(t)} \rightarrow \psi_k^{(t)}}(\psi_k^{(t)}), \forall n' \neq n\}$ and the a prior $f_{\psi_k}(\psi_k^{(t)})$, the outgoing backward message at $\psi_k^{(t)}$ can be expressed as

$$I_{\psi_k^{(t)} \rightarrow f_{\delta_{k,n}}^{(t)}}(\psi_k^{(t)}) = f_{\psi_k}(\psi_k^{(t)}) \prod_{n' \neq n} I_{f_{\delta_{k,n'}}^{(t)} \rightarrow \psi_k^{(t)}}(\psi_k^{(t)}) \\ \triangleq \sum_{q \in \mathcal{X}_d} \alpha_{k,t}^q \delta(\psi_k^{(t)} - q), \quad (49)$$

where

$$\alpha_{k,t}^q = \frac{\prod_{n' \neq n} \mathcal{CN}(\vec{m}_{\bar{x}_{k,n'}}^{(t)}; q \vec{m}_{\bar{x}_{k,n'}}^{(t-1)}, \vec{v}_{\bar{x}_{k,n'}}^{(t)} + |q|^2 \vec{v}_{\bar{x}_{k,n'}}^{(t-1)})}{\sum_{q' \in \mathcal{X}_d} \prod_{n' \neq n} \mathcal{CN}(\vec{m}_{\bar{x}_{k,n'}}^{(t)}; q' \vec{m}_{\bar{x}_{k,n'}}^{(t-1)}, \vec{v}_{\bar{x}_{k,n'}}^{(t)} + |q'|^2 \vec{v}_{\bar{x}_{k,n'}}^{(t-1)})} \quad (50)$$

With $I_{\psi_k^{(t)} \rightarrow f_{\delta_{k,n}}^{(t)}}(\psi_k^{(t)})$ and $I_{\bar{x}_{k,n}^{(t-1)} \rightarrow f_{\delta_{k,n}}^{(t)}}(\bar{x}_{k,n}^{(t-1)})$, the outgoing backward message from $f_{\delta_{k,n}}^{(t)}$ to $\bar{x}_{k,n}^{(t)}$ can be expressed as

$$I_{f_{\delta_{k,n}}^{(t)} \rightarrow \bar{x}_{k,n}^{(t)}}(\bar{x}_{k,n}^{(t)}) = \int f_{\delta_{k,n}}^{(t)}(\bar{x}_{k,n}^{(t)}, \bar{x}_{k,n}^{(t-1)}, \psi_k^{(t)}) I_{\bar{x}_{k,n}^{(t-1)} \rightarrow f_{\delta_{k,n}}^{(t)}}(\bar{x}_{k,n}^{(t-1)}) \\ \cdot I_{\psi_k^{(t)} \rightarrow f_{\delta_{k,n}}^{(t)}}(\psi_k^{(t)}) d\bar{x}_{k,n}^{(t-1)} d\psi_k^{(t)} \quad (51) \\ = \sum_{q \in \mathcal{X}} \alpha_{k,t}^q |q|^2 \mathcal{CN}(\bar{x}_{k,n}^{(t)}; q \vec{m}_{\bar{x}_{k,n}^{(t-1)}}, |q|^2 \vec{v}_{\bar{x}_{k,n}^{(t-1)}}),$$

and with $I_{\bar{x}_{k,n}^{(t)} \rightarrow f_{\delta_{k,n}}^{(t)}}(\bar{x}_{k,n}^{(t)})$ given in (43), the belief of $\bar{x}_{k,n}^{(t)}$ can be updated by

$$b(\bar{x}_{k,n}^{(t)}) = I_{f_{\delta_{k,n}}^{(t)} \rightarrow \bar{x}_{k,n}^{(t)}}(\bar{x}_{k,n}^{(t)}) I_{\bar{x}_{k,n}^{(t)} \rightarrow f_{\delta_{k,n}}^{(t)}}(\bar{x}_{k,n}^{(t)}) \\ \propto \sum_{q \in \mathcal{X}} \rho_{k,t}^q \mathcal{CN}(\bar{x}_{k,n}^{(t)}; m_{\bar{x}_{k,n}}^{(t)}, v_{\bar{x}_{k,n}}^{(t)}), \quad (52)$$

where

$$\rho_{k,t}^q = \frac{\alpha_{k,t}^q |q|^2 \mathcal{CN}(\vec{m}_{\bar{x}_{k,n}^{(t)}}; q \vec{m}_{\bar{x}_{k,n}^{(t-1)}}, \vec{v}_{\bar{x}_{k,n}^{(t)}} + |q|^2 \vec{v}_{\bar{x}_{k,n}^{(t-1)}})}{\sum_{q' \in \mathcal{X}} \alpha_{k,t}^{q'} |q'|^2 \mathcal{CN}(\vec{m}_{\bar{x}_{k,n}^{(t)}}; q' \vec{m}_{\bar{x}_{k,n}^{(t-1)}}, \vec{v}_{\bar{x}_{k,n}^{(t)}} + |q'|^2 \vec{v}_{\bar{x}_{k,n}^{(t-1)}})} \quad (53)$$

and

$$v_{k,n}^{(t)} = \left(\frac{1}{\vec{v}_{\bar{x}_{k,n}}^{(t)}} + \frac{1}{|q|^2 \vec{v}_{\bar{x}_{k,n}}^{(t-1)}} \right)^{-1}, \quad (54)$$

$$m_{k,n}^{(t)} = v_{\bar{x}_{k,n}}^{(t)} \left(\frac{\vec{m}_{\bar{x}_{k,n}}^{(t)}}{\vec{v}_{\bar{x}_{k,n}}^{(t)}} + \frac{q \vec{m}_{\bar{x}_{k,n}}^{(t-1)}}{|q|^2 \vec{v}_{\bar{x}_{k,n}}^{(t-1)}} \right). \quad (55)$$

As $I_{f_{\delta_{k,n}}^{(t)} \rightarrow \bar{x}_{k,n}}^{(t)}$ is not Gaussian, the belief $b(\bar{x}_{k,n}^{(t)})$ is not Gaussian either. With moment matching, $b(\bar{x}_{k,n}^{(t)})$ is approximated to be Gaussian to make the message tractable. Then we have

$$b^G(\bar{x}_{k,n}^{(t)}) = \text{Proj}_G \{b(\bar{x}_{k,n}^{(t)})\} \\ \triangleq \mathcal{CN}(\bar{x}_{k,n}^{(t)}; m_{\bar{x}_{k,n}}^{(t)}, v_{\bar{x}_{k,n}}^{(t)}), \quad (56)$$

where $\text{Proj}_G\{\cdot\}$ denotes the operation of Gaussian approximation, and the mean and the variance of $\bar{x}_{k,n}^{(t)}$ are given as

$$m_{\bar{x}_{k,n}}^{(t)} = \sum_{q \in \mathcal{X}} \rho_{k,t}^q m_{k,n}^{(t)}, \quad (57)$$

$$v_{\bar{x}_{k,n}}^{(t)} = \sum_{q \in \mathcal{X}} \rho_{k,t}^q (|m_{k,n}^{(t)}|^2 + v_{k,n}^{(t)}). \quad (58)$$

With $I_{\psi_k^{(t)} \rightarrow f_{\delta_{k,n}}^{(t)}}(\psi_k^{(t)})$ and $I_{\bar{x}_{k,n}^{(t)} \rightarrow f_{\delta_{k,n}}^{(t)}}(\bar{x}_{k,n}^{(t)})$, the outgoing backward message from $f_{\delta_{k,n}}^{(t)}$ to $\bar{x}_{k,n}^{(t-1)}$ can be expressed as

$$I_{f_{\delta_{k,n}}^{(t)} \rightarrow \bar{x}_{k,n}^{(t-1)}}(\bar{x}_{k,n}^{(t-1)}) = \int f_{\delta_{k,n}}^{(t)}(\bar{x}_{k,n}^{(t)}, \bar{x}_{k,n}^{(t-1)}, \psi_k^{(t)}) I_{\bar{x}_{k,n}^{(t)} \rightarrow f_{\delta_{k,n}}^{(t)}}(\bar{x}_{k,n}^{(t)}) \\ \cdot I_{\psi_k^{(t)} \rightarrow f_{\delta_{k,n}}^{(t)}}(\psi_k^{(t)}) d\bar{x}_{k,n}^{(t)} d\psi_k^{(t)} \\ = \sum_{q \in \mathcal{X}} \frac{\alpha_{k,t}^q}{|q|^2} \mathcal{CN}\left(\bar{x}_{k,n}^{(t-1)}; \frac{\vec{m}_{\bar{x}_{k,n}}^{(t)}}{q}, \frac{\vec{v}_{\bar{x}_{k,n}}^{(t)}}{|q|^2}\right). \quad (59)$$

With $I_{\bar{x}_{k,n}^{(t-1)} \rightarrow f_{\delta_{k,n}}^{(t)}}(\bar{x}_{k,n}^{(t-1)})$, the belief of $\bar{x}_{k,n}^{(t-1)}$ can be updated by

$$b(\bar{x}_{k,n}^{(t-1)}) = I_{f_{\delta_{k,n}}^{(t)} \rightarrow \bar{x}_{k,n}^{(t-1)}}(\bar{x}_{k,n}^{(t-1)}) I_{\bar{x}_{k,n}^{(t-1)} \rightarrow f_{\delta_{k,n}}^{(t)}}(\bar{x}_{k,n}^{(t-1)}) \\ \propto \sum_{q \in \mathcal{X}} \rho_{k,t-1}^q \mathcal{CN}(\bar{x}_{k,n}^{(t-1)}; m_{k,n}^{(t-1)}, v_{k,n}^{(t-1)}), \quad (60)$$

where $\rho_{k,t-1}^q = \rho_{k,t}^q$,

$$v_{k,n}^{(t-1)} = \left(\frac{|q|^2}{\vec{v}_{\bar{x}_{k,n}}^{(t)}} + \frac{1}{\vec{v}_{\bar{x}_{k,n}}^{(t-1)}} \right)^{-1}, \quad (61)$$

and

$$m_{k,n}^{(t-1)} = v_{\bar{x}_{k,n}}^{(t-1)} \left(\frac{q^H \vec{m}_{\bar{x}_{k,n}}^{(t)}}{\vec{v}_{\bar{x}_{k,n}}^{(t)}} + \frac{\vec{m}_{\bar{x}_{k,n}}^{(t-1)}}{\vec{v}_{\bar{x}_{k,n}}^{(t-1)}} \right). \quad (62)$$

Thus, $b^G(\bar{x}_{k,n}^{(t-1)})$ can be updated in the same way as (56)-(58).

Similar to (31)-(36), the outgoing backward message at $f_{z_{l,n}}^{(t)}$ can be computed as

$$I_{f_{z_{l,n}}^{(t)} \rightarrow z_{l,n}^{(t)}}(z_{l,n}^{(t)}) \propto \mathcal{CN}(z_{l,n}^{(t)}; \vec{m}_{z_{l,n}}^{(t)}, \vec{v}_{z_{l,n}}^{(t)}), \quad (63)$$

where

$$\vec{v}_{z_{l,n}}^{(t)} \approx \sum_{k=1}^K |\bar{P}_{l,k}|^2 v_{x_{k,n}}^{(t)}, \quad (64)$$

$$\vec{m}_{z_{l,n}}^{(t)} \approx \sum_{k=1}^K \bar{P}_{l,k} m_{x_{k,n}}^{(t)} - \frac{\vec{v}_{z_{l,n}}^{(t)} (y_{l,n}^{(t)} - i^{-1} \vec{m}_{z_{l,n}}^{(t)})}{\hat{\lambda}_n^{-1} + i^{-1} \vec{v}_{z_{l,n}}^{(t)}}. \quad (65)$$

Similar to (37)-(40), we can calculate $\{I_{f_{y_{l,n}}^{(t)} \rightarrow \lambda_n}^{(t)}(\lambda_n), \forall l\}$ and $\{I_{f_{y_{l,n}}^{(t-1)} \rightarrow \lambda_n}^{(t-1)}(\lambda_n), \forall l\}$. With the a prior $f_{\lambda_n}(\lambda_n)$, the belief of λ_n can be updated by

$$b(\lambda_n) = f_{\lambda_n}(\lambda_n) \prod_{l=1}^L I_{f_{y_{l,n}}^{(t)} \rightarrow \lambda_n}^{(t)}(\lambda_n) I_{f_{y_{l,n}}^{(t-1)} \rightarrow \lambda_n}^{(t-1)}(\lambda_n) \\ \propto \lambda_n^{2L-1} \exp \left\{ -\lambda_n \sum_{l=1}^L (|m_{z_{l,n}}^{(t)} - y_{l,n}^{(t)}|^2 + v_{z_{l,n}}^{(t)} \right. \\ \left. + |m_{z_{l,n}}^{(t-1)} - y_{l,n}^{(t-1)}|^2 + v_{z_{l,n}}^{(t-1)}) \right\}. \quad (66)$$

Thus, the estimation of noise precision is given by

$$\hat{\lambda}_n = \langle \lambda_n \rangle_{b_{\lambda_n}(\lambda_n)} \\ = \frac{2L}{\sum_{l=1}^L (|m_{z_{l,n}}^{(t)} - y_{l,n}^{(t)}|^2 + v_{z_{l,n}}^{(t)} + |m_{z_{l,n}}^{(t-1)} - y_{l,n}^{(t-1)}|^2 + v_{z_{l,n}}^{(t-1)})}. \quad (67)$$

The BP-MF message passing algorithm (BP-MF-MPA) for multi-device data detection is summarized in Algorithm 1. The output $\{b(\psi_k^{(t)}) = \sum_{q \in \mathcal{X}} \beta_{k,t}^q \delta(\psi_k^{(t)} - q), \forall k\}$ are used for making hard decisions on the symbols, i.e.,

$$\hat{\psi}_k = \arg \max_{\psi_k^{(t)} \in \mathcal{X}} b(\psi_k). \quad (68)$$

E. Computational Complexity

It can be seen from Algorithm 1 that, the complexity of the proposed BP-MF-MPA algorithm is dominated by the multiplication operations to update the mean and variance of the relevant messages. The complexity of active device detection is $O(NLU) + O(NU)$ per iteration and that of the non-coherent multi-device data detection is $O(NLK) + O(NK)$ per iteration.

IV. SIMULATION RESULTS

We assume a MIMO-NOMA system with parameters shown in Table III, and DQPSK modulation is employed. We observe that the BP-MF-MPA algorithms converge fast, and we set the maximum iteration number $N_{A_{\text{itr}}} = 50$ for active detection and the maximum iteration number $N_{D_{\text{itr}}} = 10$ for non-coherent multi-device data detection. The number of active devices is about 10% of the total number of devices, which are randomly selected from the users and access the channel randomly.

The rate of incorrect detection (miss or false detection) is used to evaluate the performance of active device detection. The miss detection rate and false detection rate of the proposed algorithm are shown in Fig.4 and Fig.5 respectively. It can be

Algorithm 1 BP-MF-MPA for active device detection and non-coherent multi-device data detection

Input: $\mathbf{Y}^{(t)}$, $\mathbf{Y}^{(t-1)}$, \mathbf{P} , $\{p(\gamma_u)\}$, $\{p(\psi_k^{(t)})\}$
Initialize: $\forall n, \hat{\lambda}_n = 10$; $\forall u, \hat{\gamma}_u = 1$; $\forall u, n, m_{u,n}^{(0)} = 0$;

$$\forall l, n, \bar{m}_{z_{l,n}}^{(0)} = 0, \bar{v}_{z_{l,n}}^{(0)} = 1, \bar{m}_{z_{l,n}}^{(t-1)} = 0, \bar{v}_{z_{l,n}}^{(t-1)} = 1$$

Active Device Detection:

```

1: for  $i = 1 : N_{A_{tr}}$ 
2:    $\forall u, n$ : update  $\bar{m}_{u,n}^{(i)}$ ,  $\bar{v}_{u,n}^{(i)}$  by (21) and (20);
3:    $\forall u, n$ : update  $m_{u,n}^{(i)}$ ,  $v_{u,n}^{(i)}$  by (23) and (24);
4:    $\forall l, n$ : update  $\bar{m}_{z_{l,n}}^{(i)}$ ,  $\bar{v}_{z_{l,n}}^{(i)}$  by (36) and (35);
5:    $\forall u$ : update  $\hat{\gamma}_u$  by (27);
6:   update  $\hat{\epsilon}$  by (28);
7:    $\forall l, n$ : update  $m_{z_{l,n}}^{(i)}$ ,  $v_{z_{l,n}}^{(i)}$  by (39) and (38);
8:    $\forall n$ : update  $\hat{\lambda}_n$  by (42);
9: end for
Output:  $\mathcal{I}_a = \text{find}(\{\hat{\gamma}_u\} < G_{th})$ .

```

Non-Coherent Multi-Device Data Detection

```

10: for  $i = 1 : N_{D_{tr}}$ 
11:    $\forall k, n$ : update  $\bar{m}_{k,n}^{(i)}$ ,  $\bar{v}_{k,n}^{(i)}$  by (45) and (44), and update
       $\bar{m}_{k,n}^{(i-1)}$ ,  $\bar{v}_{k,n}^{(i-1)}$  similarly;
12:    $\forall k, q$ : update  $\beta_{k,t}^q$  and  $\alpha_{k,t}^q$  by (48) and (50) respectively;
13:    $\forall k, q$ : update  $\rho_{k,t}^q$  by (53);
14:    $\forall k, n$ : update  $m_{k,n}^{(i)}$ ,  $v_{k,n}^{(i)}$  by (55) and (54), and update
       $m_{k,n}^{(i-1)}$ ,  $v_{k,n}^{(i-1)}$  by (62) and (61) respectively;
15:    $\forall k, n$ : update  $\bar{m}_{k,n}^{(i)}$ ,  $\bar{v}_{k,n}^{(i)}$  by (57) and (58), and update
       $m_{k,n}^{(i-1)}$ ,  $v_{k,n}^{(i-1)}$  similarly;
16:    $\forall l, n$ : update  $\bar{m}_{z_{l,n}}^{(i)}$ ,  $\bar{v}_{z_{l,n}}^{(i)}$  by (64) and (65), and update
       $\bar{m}_{z_{l,n}}^{(i-1)}$ ,  $\bar{v}_{z_{l,n}}^{(i-1)}$  similarly;
17:    $\forall l, n$ : update  $m_{z_{l,n}}^{(i)}$ ,  $v_{z_{l,n}}^{(i)}$  by (39) and (38), and update
       $m_{z_{l,n}}^{(i-1)}$ ,  $v_{z_{l,n}}^{(i-1)}$  similarly;
18:    $\forall n$ : update  $\hat{\lambda}_n$  by (42);
19: end for
Output:  $\forall k : b(\psi_k^{(t)}) = \sum_{q \in \mathcal{X}} \beta_{k,t}^q \delta(\psi_k^{(t)} - q)$ , based on which hard
decisions can be made.

```

TABLE III
SIMULATION PARAMETERS

Parameter	Symbol	Value
Number of devices	U	100
Number of antennas at AP	N	50,100
Number of active devices	K	$[0.1U]$
Length of spreading sequences	L	11,13

seen that with a fixed number of antennas at AP $N = 100$, the detection performance becomes better with the increase of L , as longer spreading sequences lead to smaller correlations. In addition, with a fixed length of spreading sequences $L = 13$, we examine the miss detection rate and false detection rate by varying N . As expected, a larger number of antennas lead to a better detection performance as more observations can be obtained by the receiver.

We use the bit error rate (BER) to evaluate the performance

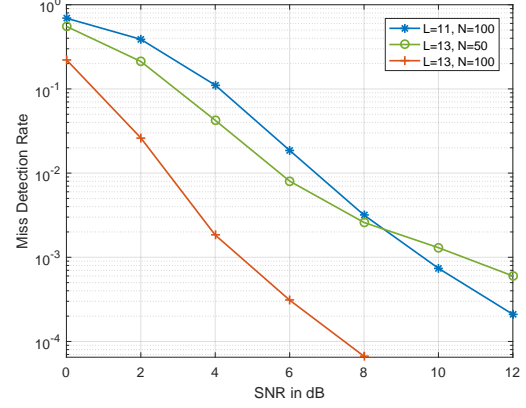


Fig. 4. Missed detection rate performance comparison.

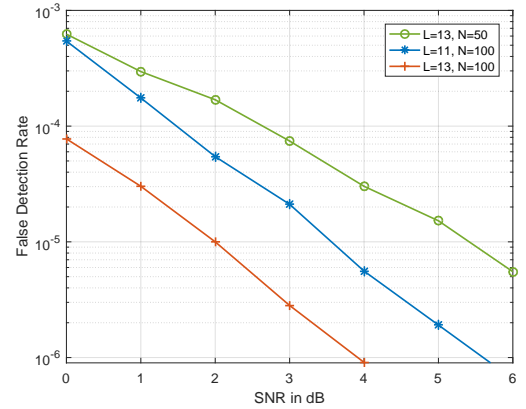


Fig. 5. False detection rate performance comparison.

of multi-device data detection. To demonstrate the superior performance of the proposed algorithm, which exploits the differential modulation constraint, we compare it with the conventional detection scheme. With the results of active device detection, the inactive devices are removed from the model. Then the estimation of $\bar{\mathbf{X}}$ becomes a conventional problem, which can be solved by using the linear minimum squared error estimator. The estimates of $\bar{\mathbf{X}}$ of two consecutive times can be obtained, which are denoted by $\bar{\mathbf{X}}^{(t)}$ and $\bar{\mathbf{X}}^{(t-1)}$. Then the demodulated symbol can be expressed as $\hat{\psi}_k = 1/N \sum_{n=1}^N \bar{x}_{k,n}^{(t)} / \bar{x}_{k,n}^{(t-1)}$, based on which hard decisions can be made. The proposed scheme is significantly different from the conventional scheme in that the estimation of $\{\psi_k\}$ is based on $\mathbf{Y}^{(t-1)}$ and $\mathbf{Y}^{(t)}$ directly and jointly.

The BER performance of the proposed scheme and the conventional scheme with respect to signal-to-noise ratios (SNRs) is shown in Fig. 6, where the length of spreading sequence $L = 11$ and the number of antennas at AP $N = 100$. As a performance benchmark, the ID-aided MPA scheme, where the common support is perfectly known, is also included. It can be seen that the gap between the proposed scheme and the ID-aided MPA scheme is about 2dB at the BER of 10^{-5} . In addition, compared with the conventional scheme, the proposed scheme can improve the BER performance significantly

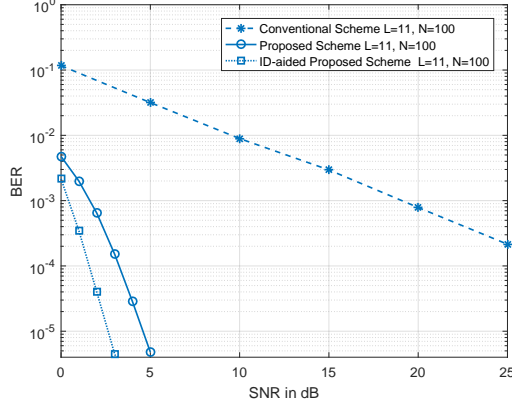


Fig. 6. BER performance comparison of multi-device data detection, where $L = 11$ and $N = 100$.

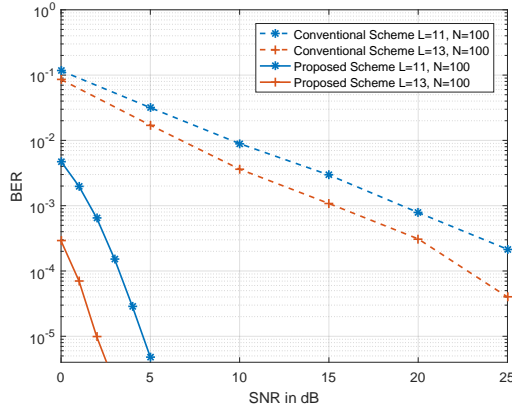


Fig. 7. BER performance comparison of multi-device data detection for different L , where $N = 100$.

over the entire SNR range, because the proposed BP-MF-MPA algorithm make full use of the differential constrain information.

With different L , the BER performance of the two schemes is shown in Fig. 7. It can be observed that, the schemes with $L = 13$ delivers better BER performance than those with $L = 11$. This is because longer spreading sequence can reduce the cross-correlation of the spreading sequences, which brings down the multi-user interference. Finally, we examine the BER performance of the schemes by varying the number of antennas N equipped at AP, and the results are shown in Fig. 8. It can be seen that, with the increase of N , the BER performance is improved as expected.

V. CONCLUSION

In this paper, we have investigated the design of grant-free MIMO-NOMA system for machine type communications with the aim to achieve high efficiency and low latency. In particular, differential modulation is employed so that the costly channel estimation in MIMO-NOMA can be bypassed, and the use of long training signals are avoided. The receiver needs to perform active device detection and multi-device detection. We have designed message passing based SBL algorithm

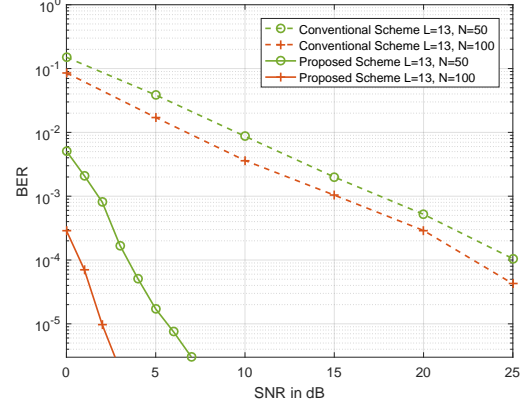


Fig. 8. BER performance comparison of multi-device data detection for different N , where $L = 13$.

to solve the active device detection problem. We have also developed message passing based non-coherent multi-device data detector, where the differential modulation is exploited as a constraint in the detection, leading to significant performance improvement compared to conventional demodulation scheme. Both active device detection and multi-device data detection are performed symbol-by-symbol, which allow highly flexible transmission of the IoT devices. Simulation results verified the effectiveness of the proposed detectors.

APPENDIX A

DERIVATIONS OF (21) AND (36)

A. Derivation of (21)

$$\begin{aligned}
 \vec{m}_{x_{u,n}}^{(i)} &= \vec{v}_{x_{u,n}}^{(i)} \left(\sum_{l=1}^L \frac{\vec{m}_{x_{u,n,l}}^{(i)}}{\vec{v}_{x_{u,n,l}}^{(i)}} \right) \\
 &\approx \vec{v}_{x_{u,n}}^{(i)} \sum_{l=1}^L \frac{P_{l,u}^H \left(y_{l,n}^{(i)} - \vec{m}_{z_{l,n}}^{(i)} + P_{l,u} \vec{m}_{x_{u,n,l}}^{(i)} \right)}{\hat{\lambda}_n^{-1} + \vec{v}_{z_{l,n}}^{(i)}} \\
 &\stackrel{(33)}{\approx} \vec{v}_{x_{u,n}}^{(i)} \sum_{l=1}^L \frac{P_{l,u}^H \left(y_{l,n}^{(i)} - \vec{m}_{z_{l,n}}^{(i)} \right)}{\hat{\lambda}_n^{-1} + \vec{v}_{z_{l,n}}^{(i)}} \\
 &\quad + \vec{v}_{x_{u,n}}^{(i)} \sum_{l=1}^L \frac{|P_{l,u}|^2 \left(m_{x_{u,n}}^{(i)} - v_{x_{u,n}}^{(i)} \frac{\vec{m}_{x_{u,n,l}}^{(i)}}{\vec{v}_{x_{u,n,l}}^{(i)}} \right)}{\hat{\lambda}_n^{-1} + \vec{v}_{z_{l,n}}^{(i)}} \\
 &\stackrel{(20)(32)}{\approx} \vec{v}_{x_{u,n}}^{(i)} \sum_{l=1}^L \frac{P_{l,u}^H \left(y_{l,n}^{(i)} - \vec{m}_{z_{l,n}}^{(i)} \right)}{\hat{\lambda}_n^{-1} + \vec{v}_{z_{l,n}}^{(i)}} + m_{x_{u,n}}^{(i)} \\
 &\quad - \vec{v}_{x_{u,n}}^{(i)} \sum_{l=1}^L \frac{|P_{l,u}|^2 \vec{m}_{x_{u,n,l}}^{(i)}}{\hat{\lambda}_n^{-1} + \vec{v}_{z_{l,n}}^{(i)}} \\
 &\approx \vec{v}_{x_{u,n}}^{(i)} \sum_{l=1}^L \frac{P_{l,u}^H \left(y_{l,n}^{(i)} - \vec{m}_{z_{l,n}}^{(i)} \right)}{\hat{\lambda}_n^{-1} + \vec{v}_{z_{l,n}}^{(i)}} + m_{x_{u,n}}^{(i)}.
 \end{aligned}$$

B. Derivation of (36)

$$\begin{aligned}
 \bar{m}_{z,l,n}^{(i)} &= \sum_{u=1}^U P_{l,u} \bar{m}_{x,u,n,l}^{(i)} \\
 &\stackrel{(33)}{\approx} \sum_{u=1}^U P_{l,u} \left(m_{x,u,n}^{(i)} - v_{x,u,n}^{(i)} \frac{\bar{m}_{x,u,n,l}^{(i)}}{v_{x,u,n,l}^{(i)}} \right) \\
 &\stackrel{(15)(16)}{\approx} \sum_{u=1}^U \left(P_{l,u} m_{x,u,n}^{(i)} - \frac{v_{x,u,n}^{(i)} |P_{l,u}|^2 (y_{l,n}^{(i)} - i^{-1} \bar{m}_{z,l,n}^{(i)})}{\hat{\lambda}_n^{-1} + i^{-1} \bar{v}_{z,l,n}^{(i)}} \right) \\
 &\stackrel{(35)}{\approx} \sum_{u=1}^U P_{l,u} m_{x,u,n}^{(i)} - \frac{\bar{v}_{z,l,n}^{(i)} (y_{l,n}^{(i)} - i^{-1} \bar{m}_{z,l,n}^{(i)})}{\hat{\lambda}_n^{-1} + i^{-1} \bar{v}_{z,l,n}^{(i)}}.
 \end{aligned}$$

REFERENCES

- [1] F. Boccardi, R. W. Heath, A. Lozano, T. L. Marzetta, and P. Popovski, "Five disruptive technology directions for 5G," *IEEE Communications Magazine*, vol. 52, no. 2, pp. 74–80, Feb. 2014.
- [2] H. Tullberg, P. Popovski, Z. Li, M. A. Uusitalo, A. Hoglund, O. Bulakci, M. Fallgren, and J. F. Monserrat, "The METIS 5G system concept: Meeting the 5G requirements," *IEEE Communications Magazine*, vol. 54, no. 12, pp. 132–139, Dec. 2016.
- [3] M. R. Palattella, M. Dohler, A. Grieco, G. Rizzo, J. Torsner, T. Engel, and L. Ladid, "Internet of Things in the 5G Era : Enablers, Architecture, and Business Models," *IEEE Journal on Selected Areas in Communications*, vol. 34, no. 3, pp. 510–527, Mar. 2016.
- [4] M. T. Islam, M. T. Abd-elhamid, and S. Akl, "A survey of access management techniques in machine type communications," *IEEE communications Magazine*, vol. 52, no. 4, pp. 74–81, May 2014.
- [5] C. Bockelmann, N. Pratas, H. Nikopour, K. Au, T. Svensson, C. Stefanovic, P. Popovski, and A. Dekorsy, "Massive machine-type communications in 5G: Physical and MAC-layer solutions," *IEEE Communications Magazine*, vol. 54, no. 9, pp. 59–65, Sept. 2016.
- [6] Y. Saito, Y. Kishiyama, A. Benjebbour, T. Nakamura, A. Li, and K. Higuchi, "Non-Orthogonal Multiple Access (NOMA) for Cellular Future Radio Access," in *Proc. of the IEEE 77th Vehicular Technology Conference (VTC Spring)*, Jun. 2013, pp. 1–5.
- [7] L. Dai, B. Wang, Y. Yuan, S. Han, I. Chih-Lin, and Z. Wang, "Non-orthogonal multiple access for 5G: solutions, challenges, opportunities, and future research trends," *IEEE Communications Magazine*, vol. 53, no. 9, pp. 74–81, Sept. 2015.
- [8] M. Shirvanimoghaddam, M. Dohler, and S. J. Johnson, "Massive Non-Orthogonal Multiple Access for Cellular IoT: Potentials and Limitations," *IEEE Communications Magazine*, vol. 55, no. 9, pp. 55–61, Sep. 2017.
- [9] Q. Wang, R. Zhang, L. Yang, and L. Hanzo, "Non-Orthogonal Multiple Access: A Unified Perspective," *IEEE Wireless Communications*, vol. 25, no. 2, pp. 10–16, Apr. 2018.
- [10] M. Vaezi, Z. Ding, and H. V. Poor, *Multiple access techniques for 5G wireless networks and beyond*. Springer, 2019.
- [11] Y. Zhang, Z. Yuan, Q. Guo, Z. Wang, J. Xi, and Y. Li, "Bayesian receiver design for grant-free noma with message passing based structured signal estimation," *IEEE Transactions on Vehicular Technology*, vol. 69, no. 8, pp. 8643–8656, 2020.
- [12] Y. Zhang, Q. Guo, Z. Wang, J. Xi, and N. Wu, "Block sparse bayesian learning based joint user activity detection and channel estimation for grant-free noma systems," *IEEE Transactions on Vehicular Technology*, vol. 67, no. 10, pp. 9631–9640, 2018.
- [13] Y. Huang, C. Zhang, J. Wang, Y. Jing, L. Yang, and X. You, "Signal Processing for MIMO-NOMA: Present and Future Challenges," *IEEE Wireless Communications*, vol. 25, no. 2, pp. 32–38, 2018.
- [14] Q. Sun, S. Han, C. I., and Z. Pan, "On the Ergodic Capacity of MIMO NOMA Systems," *IEEE Wireless Communications Letters*, vol. 4, no. 4, pp. 405–408, 2015.
- [15] Z. Ding, R. Schober, and H. V. Poor, "A General MIMO Framework for NOMA Downlink and Uplink Transmission Based on Signal Alignment," *IEEE Transactions on Wireless Communications*, vol. 15, no. 6, pp. 4438–4454, 2016.
- [16] M. Zeng, A. Yadav, O. A. Dobre, G. I. Tsiropoulos, and H. V. Poor, "Capacity Comparison Between MIMO-NOMA and MIMO-OMA With Multiple Users in a Cluster," *IEEE Journal on Selected Areas in Communications*, vol. 35, no. 10, pp. 2413–2424, 2017.
- [17] W. Shin, M. Vaezi, B. Lee, D. J. Love, J. Lee, and H. V. Poor, "Coordinated Beamforming for Multi-Cell MIMO-NOMA," *IEEE Communications Letters*, vol. 21, no. 1, pp. 84–87, 2017.
- [18] L. Liu, Y. Chi, C. Yuen, Y. L. Guan, and Y. Li, "Capacity-Achieving MIMO-NOMA: Iterative LMMSE Detection," *IEEE Transactions on Signal Processing*, vol. 67, no. 7, pp. 1758–1773, 2019.
- [19] A. S. de Sena, F. R. M. Lima, D. B. da Costa, Z. Ding, P. H. J. Nardelli, U. S. Dias, and C. B. Papadias, "Massive MIMO-NOMA Networks With Imperfect SIC: Design and Fairness Enhancement," *IEEE Transactions on Wireless Communications*, vol. 19, no. 9, pp. 6100–6115, 2020.
- [20] B. Fontana da Silva, C. A. Azurdia Meza, D. Silva, and B. F. Uchôa-Filho, "Exploiting spatial diversity in overloaded MIMO LDS-OFDM multiple access systems," in *Proc. of 2017 IEEE 9th Latin-American Conference on Communications (LATINCOM)*, 2017, pp. 1–6.
- [21] Z. Pan, W. Liu, J. Lei, J. Luo, L. Wen, and C. Tang, "Multi-Dimensional Space-Time Block Coding Aided Downlink MIMO-SCMA," *IEEE Transactions on Vehicular Technology*, vol. 68, no. 7, pp. 6657–6669, 2019.
- [22] L. Liu, C. Yuen, Y. L. Guan, Y. Li, and C. Huang, "Gaussian Message Passing for Overloaded Massive MIMO-NOMA," *IEEE Transactions on Wireless Communications*, vol. 18, no. 1, pp. 210–226, 2019.
- [23] H. V. Cheng, E. Björnson, and E. G. Larsson, "Performance Analysis of NOMA in Training-Based Multiuser MIMO Systems," *IEEE Transactions on Wireless Communications*, vol. 17, no. 1, pp. 372–385, 2018.
- [24] J. Ma, C. Liang, C. Xu, and L. Ping, "On orthogonal and superimposed pilot schemes in massive mimo noma systems," *IEEE Journal on Selected Areas in Communications*, vol. 35, no. 12, pp. 2696–2707, 2017.
- [25] F. R. Kschischang, B. J. Frey, and H.-A. Loeliger, "Factor graphs and the sum-product algorithm," *IEEE Transactions on information theory*, vol. 47, no. 2, pp. 498–519, Feb. 2001.
- [26] E. P. Xing, M. I. Jordan, and S. Russell, "A generalized mean field algorithm for variational inference in exponential families," in *Proc. of the 19th conference on Uncertainty in Artificial Intelligence*, Aug. 2003, pp. 583–591.
- [27] J. Winn and C. M. Bishop, "Variational message passing," *Journal of Machine Learning Research*, vol. 6, no. Apr., pp. 661–694, 2005.
- [28] R. Frank, S. Zadorff, and R. Heimiller, "Phase shift pulse codes with good periodic correlation properties (corresp.)," *IRE Transactions on Information Theory*, vol. 8, no. 6, pp. 381–382, Oct. 1962.
- [29] D. Chu, "Polyphase codes with good periodic correlation properties (corresp.)," *IEEE Transactions on information theory*, vol. 18, no. 4, pp. 531–532, Jul. 1972.
- [30] M. Luo, Q. Guo, M. Jin, Y. C. Eldar, D. Huang, and X. Meng, "Unitary approximate message passing for sparse bayesian learning," *IEEE Transactions on Signal Processing*, vol. 69, pp. 6023–6039, 2021.
- [31] C. Wei, H. Liu, Z. Zhang, J. Dang, and L. Wu, "Near-optimum sparse channel estimation based on least squares and approximate message passing," *IEEE Wireless Communications Letters*, vol. 6, no. 6, pp. 754–757, 2017.